Int. J. Nonlinear Anal. Appl. 12 (2021) No. 2, 583-601
ISSN: 2008-6822 (electronic)
http://dx.doi.org/10.22075/ijnaa.2020.19429.2078

Nonlinear instability analysis of a vertical cylindrical magnetic sheet

Galal Moatimid[a], Yusry El-Dib[a], Marwa Zekry[b,*]

[a]Department of Mathematics, Faculty of Education, Ain Shams University, Roxy, Cairo, Egypt
[b]Department of Mathematics and Computer Science, Faculty of Science, Beni-Suef University, Egypt

(Communicated by Mugur Alexandru Acu)

Abstract

This paper concerns with the nonlinear instability analysis of double interfaces separated three perfect, incompressible cylindrical magnetic fluids. The cylindrical sheet is acted upon by an axial uniform magnetic field. The current nonlinear approach depends mainly on solving the linear governing equations of motion and is subjected to the appropriate nonlinear boundary conditions. This procedure resulted in two nonlinear characteristic equations governed by the behavior of the interface's deflection. By means of the Taylor expansion, together with the multiple time scales, technique, the stability analysis of linear as well as the nonlinear is achieved. The linear stability analysis reveals a quadratic dispersion equation in the square of growth rate frequency of the surface wave. On the other hand, the nonlinear analysis is accomplished by a coupled nonlinear Schrödinger equation of the evolution amplitudes of the surface waves. The stability criteria resulted in a polynomial of the eleventh degree in the square of the magnetic field strength, together with resonance transition curves. Several special cases are reported upon appropriate data choices. The stability criteria are numerically discussed, at which regions of stability and instability are identified. In the stability profile, the magnetic field intensity is plotted versus the wave number. The influences of the parameters on the stability are addressed. The nonlinear stability approach divides the phase plane into several parts of stability/instability. The nonlinear stability shows an in contrast mechanism of the role of the sheet thickness.

Keywords: Nonlinear Stability Analysis; Magnetic Fluids, Multiple Time Scales, Coupled Nonlinear Schrödinger Equations
2010 MSC: Primary 76E25; Secondary 34E13.

*Corresponding author
Email addresses: gal_moa@hotmail.com (Galal Moatimid), yusryeldib52@hotmail.com (Yusry El-Dib), marwa.zekry@science.bsu.edu.eg (Marwa Zekry)

Received: January 2020 *Accepted:* April 2020

1. Introduction

Berkovski, and Bashtovoy [1] introduced a handbook on the topic of ferrofluid (FF). Throughout this book, they have explained the basic principles, significance in regard to its theory in different practical situations. They showed that the core of magnetic fluid technology is based on liquid and magnetic phenomena. Furthermore, they discussed the fundamental characteristics of the magnetic fluid along with measurement techniques. Magnetic nano-particle has received great attention owing to their potential usefulness in magnetic resonance imaging or colloidal mediators for cancer magnetic hyperthermia. Rheinländer et al.[2] presented a simple magnetic method for the fractionation of FF. It was shown that their technique separates the magnetic nano-particle according to the magnetic moments. Furthermore, the method of fractionates of different magnetic fluids successfully has good reproducibility. Therefore, the particles obtained by this technique became better suited for a number of applications. Along with the applications in medicine and biotechnology, Chaniyilparampu et al. [3] showed that FF could be successfully directed to the tumors in about one half of the patients. Moreover, they indicated the potential of using the magnetic particles as an effective drug delivery system, in order to relieve patients of unwanted side effects of anticancer drugs. Therefore, Mornet et al. [4] introduced a review on this topic. Furthermore, a special emphasis was made on magnetic nano-particle requirements from a physical point of view. Ganguly et al. [5] performed experimental and numerical investigations of magnetically induced localization of FF and its subsequent dispersion in a forced flow. They found that the FF accumulation behaves as a solid obstacle in the flow. Moreover, their analysis provides meaningful information about FF transport for various magnetic drug targeting applications. Scherer, and Neto [6] reviewed the general classification and the main properties of the FF together with theoretical models. In addition, they considered the stability of a FF in terms of various forces and torques on the magnetic particles. Furthermore, their work included a few of many technological applications. Among these applications, they selected the doping of liquid crystals and added many comments for future research on the properties of FF.

A significant review of the hydrodynamic stability of the Rayleigh Taylor and Kelvin-Helmholtz instabilities had been reported throughout Chandrasekhar's [7] pioneer book. El Shehawey et al. [8] studied the electrohydrodynamic (EHD) stability of a fluid layer that imbedded between two different fluids. Their perfect fluid system was influenced, only, by gravitational forces together with the tangential electric field. They showed that the tangential electric field plays a stabilizing role in the stability picture, it may be used to suppress the instability of the system at a certain wave number. Their stability analysis resulted in two simultaneous linear second-order differential equations. Mohamed et al. [9] introduced the same problem that was given in Ref [8] but in the case of a periodic electric field. In this case, they obtained two simultaneous ordinary differential equations of the Matheieu type. They used the multiple time scale technique to judge the stability criteria. They showed that the tangential periodic field cannot stabilize a system that is unstable under a uniform electric field. Mohamed et al. [10] studied the EHD of two interfaces separating three fluid phases. They considered two cases; the case of the absence of surface charges together with that in its presence. They showed that the field is still has a destabilizing influence, but this influence is partially shielded in some situations. El-Dabe et al. [11] studied the EHD stability of two cylindrical interfaces acted upon by a periodic tangential magnetic field. Two simultaneous ordinary differential equations of the Mathieu type were obtained. They utilized the multiple time scales method to judge the stability criteria of the system. They found that the uniform electric field has a stabilizing effect, meanwhile, the periodic one has a stabilizing influence except at some resonance points. Actually, the current manuscript given an extension to our previous work [11]. It aims to investigate the nonlinear stability analysis of the double cylindrical interfaces. For simplicity, the present study considers only a perfect fluid without any additional parameters except the gravitational forces as well as an axial uniform magnetic field. El-Dib and Matoog [12] investigated the problem by electro-viscoelastic Kelvin-Helmholtz waves of three phase Maxwellian fluids under the influence of a periodic normal electric field in the absence of surface charges. They used the symmetric and anti-symmetric modes in their analysis. Moreover, they indicated that the thickness of the horizontal layer, as well as the frequency of the layer, played a destabilizing role in the stability picture. Moatimid et al. [13] investigated the influence of an axial periodic field on streaming flows throughout three coaxial infinitely cylinders. Recently, Moatimid et al. [14] studied the linear stability analysis of a vertical cylindrical sheet. Their boundary-value problem resulted in a coupled second-order damped differential equation with complex coefficients. Utilizing the symmetric and anti-symmetric modes, they combined these equations to obtain a single dispersion equation. Therefore, they acquired the stability criteria analytically and confirmed them numerically.

Various natural and scientific phenomena are typically modeled and illustrated in view of differential equations. In material science, there are many fundamental equations for portraying a quantum mechanical behavior; for example, see Arnold [15]. In this work, Arnold [15] showed that the transparent boundary conditions for the transient Schrödinger equation -in a certain domain- can be derived under the assumption that the given uniform potential lies outside this domain. Among them, the most important equation is the nonlinear Schrödinger equation which is used to elucidate the changes of quantum systems with time. Furthermore, this equation has many applications in various fields of the physical sciences; for instance, in the configuration of optoelectronic gadgets, in studying the electromagnetic wave proliferation, quantum flow computations, underwater acoustics, signal propagation in optical fibers, and many physical nonlinear systems having instability problems; for an example, see Levy's book [16]. Throughout this book, Levy presented the application of parabolic equation methods in electromagnetic wave propagation. These powerful numerical techniques have become a dominant tool for assessing clear-air and terrain effects on radio wave propagation and are growing increasingly popular for solving scattering problems. This book gives a mathematical background to parabolic equation modeling and describes simple parabolic equation algorithms before progressing to more advanced topics such as domain truncation. Recently, Arora et al. [17] developed a hybrid scheme for solving the nonlinear Schrödinger equation in one as well as two dimensions. Their approach reduced the nonlinear equation into a set of ordinary differential equations. By means of the modified Runge-Kutta technique, they solved these equations numerically. Furthermore, they found that the numerical results are in good agreement with the results available in the literature.

Several authors discussed the nonlinear analysis using the method of multiple time scales. Nayfeh [18] utilized this method to drive two partial differential equations that describe the evolution of two-dimensional wave-packets of the interface between two semi-infinite perfect fluids. These equations are combined to yield two alternate nonlinear Schrödinger equations. By making use of these equations, the stability criteria were achieved. Elhefnawy [19] studied the nonlinear stability analysis of the Rayleigh Taylor instability of two superposed magnetic fluids. He showed that the evolution amplitude of the surface wave is governed by a nonlinear Ginzburg-Landau equation. Therefore, the stability criteria were discussed both analytically and numerically. The nonlinear stability of a cylindrical interface between two fluids was investigated by Lee [20]. Throughout his nonlinear analysis, a nonlinear Ginzburg–Landau was obtained. Therefore, the regions of stability and instability were addressed. Zakaria [21] investigated the nonlinear stability of two superposed magnetic fluids in the presence of an oblique magnetic field. His analysis revealed Schrödinger and Klein–Gordon equations. The existing conditions of Stokes waves with their instability conditions were combined to judge general criteria. He obtained the properties of the existence of instability. These conditions were discussed analytically and graphically. El-Dib [22] extended Nayfeh's approach [18] to derive the nonlinear stability criteria of double interfaces. The analysis revealed the case of the uniform as well as periodic external fields. His technique resulted in two Schrödinger equations, by combining them, the stability criteria were obtained. A weakly nonlinear instability of the surface waves propagating between two visco-elastic cylindrical flows was investigated by Moatimid [23]. Typically, a nonlinear Schrödinger equation with complex coefficients was obtained. Therefore, the regions of stability and instability were identified for the wave train disturbances. Elhefnawy et al. [24] studied the nonlinear instability of finite cylindrical conducting fluids under the effect of a radial electric field. They found that the evolution of the amplitude of the surface wave was governed by two partial differential equations. Following Nayfeh's approach [18], they derived two alternate nonlinear Schrödinger equations. Therefore, the stability criteria were analytically discussed and confirmed numerically. Recently, Moatimid et al. [25] investigated the nonlinear instability of a cylindrical interface between two magnetic fluids in porous media. The coupling of the Laplace transforms and homotopy perturbation techniques were adopted to obtain an approximate analytical solution of the interface profile. The nonlinear stability analysis resulted in two levels of solvability conditions. By means of these conditions, a Ginzburg-Landau equation was conducted.

To our knowledge, the first treatment of the capillary stability of a hollow cylinder, i. e., a liquid bounded by two cylindrical surfaces had been performed by Dumbleton and Hermans [26]. As per the authors' knowledge, it is for the first time to analyze the nonlinear stability analysis of double interfaces. Therefore, the current investigation deals with the investigation of the nonlinear stability analysis of double interfaces. An axial uniform magnetic field stength is acted upon on a vertical magnetic cylindrical shell. The case of a periodic field will be considered in a subsequent paper. So, the current manuscript gives an extension to our previous work [11] to analyze the nonlinear stability analysis of a cylindrical sheet between two interfaces. For simplicity, this study is done without any additional parameters except an axial uniform magnetic field and the gravitational forces. The problem meets its importance from practical interest of a geophysical and industrial point of view. Typically, as given in our previous works; for instance, see Refs[23, 25], the following approach is based mainly on solving the linear equations of motion along with the corresponding nonlinear boundary conditions. The procedure yields nonlinear characteristic equations of the deflection of the interfaces. Following our previous work [22], a coupled nonlinear Schrödinger equation is obtained. Therefore, the stability criteria are achieved in the linear as well as nonlinear approaches. Furthermore, in light of the numerical estimations, the regions of stability/instability are addressed. To clarify the manuscript, the rest of the paper is organized as follows: Section 2 is devoted to the methodology of the problem. In this Section, the equations of motion and the appropriate nonlinear boundary conditions are presented. The linear stability analysis is drawn in Section 3. The nonlinear stability approach and, hence, the derivation of the coupled nonlinear Schrödinger equations are introduced in Section 4. Finally, concluding remarks are summarized in Section 5.

2. Methodology of the Problem

Vertical cylindrical flows consist of three parallel perfect, incompressible magnetic fluids are considered. Throughout this formulation the subscripts 1,2 and 3 denote the parameters that associated to the inner, middle and outer fluids, respectively. In the undisturbed state, the three fluids are separated by two coaxial cylindrical interfaces whose radii are $r = R_1$and $r = R_2$. Therefore, the two cylindrical surfaces that form the boundaries of the liquid are circular and concentric. The inner, middle and outer liquids have the uniform densitiesρ_1, ρ_2 andρ_3. The effect of the viscosity of the liquids in the inner, middle and outer the cylindrical sheet is neglected. Simultaneously, they have,

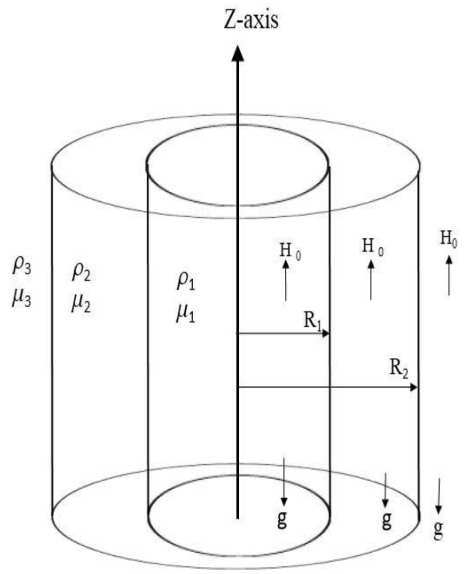

Figure 1: Sketch of the model in the undisturbed state.

in order, the magnetic permeability's μ_1, μ_2 and μ_3, respectively. The three fluids are assumed to be affected by an axial uniform magnetic field of strength H_0. For the reason illustrated below, the disturbance is assumed to have a cylindrical symmetry. Actually, the magnetic field is implemented along the positive $z-$direction. Moreover, for simplicity, no surface currents are assumed to be present at the interfaces. The gravitational acceleration g, along the negative $z$direction is, also, taken into consideration. For more convenience, we work with the cylindrical coordinates (r, θ, z). Typically, in the equilibrium state, the $z-$axis represents the axis of symmetry of the system. It is clear that, in this state, the pressure of the inner liquid, at which $r < R_1$ is larger than that of $r > R_2$, the difference being $T_1/R_1 + T_2/R_2$, where T_1 , and T_2 are the amounts of the surface tension at the inner and outer surface, respectively. It is assumed that this pressure difference remains constant during the disturbance. The physical model is sketched in Fig. 1.

Typically, as given throughout the pioneer book of Chandrasekhar [7], the liquid jet is stable for all the asymmetric modes $m \neq 0$, but it becomes unstable at the axisymmetric mode $m = 0$. Consequently, the most interesting mode of disturbance is the axisymmetric mode. Therefore, from now on, the case of $m = 0$ is only considered. The disturbed cylinder, especially considering the Fourier component with the wave number k and the cylindrical symmetry, the inner and outer surfaces, is given by

$$r = R_1 + \eta(z, t) \tag{2.1a}$$
$$r = R_2 + \xi(z, t), \tag{2.1b}$$

here $\eta(z; t)$ and $\xi(z, t)$ are a general unknown function which represents the surface deflection behavior.

Therefore, after a small departure from the equilibrium state, the interface profiles may be expressed as:

$$S_1(r, z; t) = r - R_1 - \eta(z, t) \tag{2.2a}$$
$$S_2(r, z; t) = r - R_2 - \xi(z, t), \tag{2.2b}$$

Therefore, the unit outward normal vector of the interfaces may be written as:

$$\underline{n}_1 = \nabla S_1 / |\nabla S_1| = (\underline{e}_r - \eta_z\, \underline{e}_z)(1+\eta_z^2)^{-1/2} \tag{2.3a}$$

$$\underline{n}_2 = \nabla S_2 / |\nabla S_2| = (\underline{e}_r - \xi_z\, \underline{e}_z)(1+\xi_z^2)^{-1/2}, \tag{2.3b}$$

here $\underline{e}_r$ and $\underline{e}_z$ are unit vectors along the $r-$ and $z-$directions, respectively.

The governing equations of motion of an incompressible fluid may be written as:

$$\left(\frac{\partial \underline{v}_j}{\partial t} + (\underline{v}_j.\nabla)\underline{v}_j\right) = -\frac{1}{\rho_j}\nabla P_j - g\underline{e}_z \qquad j = 1, 2, 3, \tag{2.4}$$

where $v_j = v_j(r, z; t)$ is the fluid velocity and P_j represents the pressure.

The zero-order solution of Eq. (2.4) yields

$$P_{0j} = -\rho_j g z + \lambda_j, \tag{2.5}$$

where λ_j is an arbitrary integration constant.

As shown in the formulation of the problem, the fluids are assuming as perfect flows. Therefore, one may assume that the fluids are being irrotational flows. It follows that, the perturbed velocity may be written as

$$\underline{v}_j = -\nabla\varphi_j = -\frac{\partial \varphi_j}{\partial r}\underline{e}_r - \frac{\partial \varphi_j}{\partial z}\underline{e}_z. \tag{2.6}$$

Because of the incompressibility condition, the potential function $\varphi_j(r, z; t)$ must satisfy the following Laplace equation:

$$\nabla^2\varphi_j = 0, \tag{2.7}$$

and

$$\varphi_j(r, z; t) = \hat{\varphi}_j(r; t)e^{ikz} + c.c. \tag{2.8}$$

here $c.c.$ represents the complex conjugate of the preceding term.

The solution of the Laplace's equation is then become

$$\hat{\varphi}_1(r; t) = A_1(t) I_0(kr), \tag{2.9a}$$

$$\hat{\varphi}_2(r; t) = \left(A_2(t) I_0(kr) + B_2(t) K_0(kr)\right), \tag{2.9b}$$

$$\hat{\varphi}_3(r; t) = B_3(t) K_0(kr), \tag{2.9c}$$

where $A_1(t)$, $A_2(t)$, $B_1(t)$ and $B_2(t)$ are arbitrary time-dependent functions to be evaluated in light of the appropriate nonlinear boundary conditions. Moreover, $I_0(kr)$ and $K_0(kr)$ represent the modified Bessel functions of the first and second kinds, respectively.

The integration of the linear equation of motion (2.4) resulted in the distribution function of the pressure as given by

$$P_j = \rho_j \frac{\partial \varphi_j}{\partial t}. \tag{2.10}$$

On the other hand, in accordance with the Maxwell equations; see for instance, Melcher [27], for the quasi-static approximation, on neglecting the influence of the electric field, they may be written as

$$\nabla.\mu_j \underline{H}_j = 0, \tag{2.11}$$

and

$$\nabla \times \underline{H}_j = \underline{0}. \tag{2.12}$$

As given in the formulation of the problem, no surface currents are assumed to be present at the surface of separation.

Therefore, the magnetic field may be expressed in terms of the scalar magneto-static potentials $\psi_j(r, z; t)$, i.e., $\underline{H}_j = -\nabla\psi_j(r, z; t)$ such that the total perturbed magnetic fields can be expressed as:

$$\underline{H}_j = -\frac{\partial\psi_j}{\partial r}\underline{e}_r - \left(\frac{\partial\psi_j}{\partial z} - H_0\right)\underline{e}_z. \tag{2.13}$$

The combination of equations (2.11) and (2.13) yields

$$\nabla^2\psi_j = 0. \tag{2.14}$$

As expressed previously in Eq. (2.8), the magnetic potentials may be written as:

$$\hat{\psi}_1(r; t) = C_1(t)I_0(kr), \tag{2.15a}$$

$$\hat{\psi}_2(r; t) = C_2(t)I_0(kr) + D_2(t)K_0(kr), \tag{2.15b}$$

$$\hat{\psi}_3(r; t) = D_3(t)K_0(kr), \tag{2.15c}$$

where $C_1(t)$, $C_2(t)$, $D_2(t)$ and $D_3(t)$ are arbitrary time-dependent functions to be evaluated by using the appropriate nonlinear boundary conditions.

2.1. Nonlinear Boundary Conditions

The general solutions of the velocity and magnetic potential distributions, as given in equations (2.9) and (2.15), must satisfy the appropriate nonlinear boundary conditions.

2.1.1. At the Free Interfaces $r = R_1 + \eta(z; t)$ and $r = R_2 + \xi(z; t)$

1-The conservation of mass across the interface, which is so called the kinematic condition, yields

$$\frac{DS_1}{Dt} = 0 \qquad \text{at} \qquad r = R_1 + \eta(z; t) \tag{2.16}$$

$$\frac{DS_2}{Dt} = 0 \qquad \text{at} \qquad r = R_2 + \xi(z; t) \tag{2.17}$$

here D/Dt represents the material derivative operator.
2-The jump of the tangential components of the magnetic is continuous at the interface yield

$$\underline{n}_j \times \left\|\underline{H}_j\right\| = \underline{0}.\, j = 1, 2, \tag{2.18}$$

where $\|*\| = *_2 - *_1$ denotes to the jump of the external and internal fluid layers, respectively.
3- The jump of the normal components of the magnetic is continuous at the interface give

$$\underline{n}_j. \left\|\mu_j\,\underline{H}_j\right\| = 0. \qquad j = 1, 2, \tag{2.19}$$

At this stage, on substituting from equations (2.9) and (2.15) into equations (2.16)-(2.19), one finds the special solutions which are consistent with the foregoing nonlinear boundary conditions. They can be written as follows:

$$\varphi_1 = -\frac{\eta_t I_0(x)}{k\,\left(I_1(a) - iI_0(a)\eta_z\right)}, \tag{2.20}$$

$$\varphi_2 = \frac{\eta_t\left(N_{xb} - iW_{bx}\xi_z\right) - \xi_t\left(N_{xa} - iW_{ax}\eta_z\right)}{k\,\left(L_{ba} + iN_{ab}\eta_z + \xi_z\left(W_{ba}\eta_z - iN_{ba}\right)\right)}, \tag{2.21}$$

$$\varphi_3 = \frac{\xi_t K_0(x)}{k\ (K_1(b) + iK_0(b)\xi_z)}, \tag{2.22}$$

$$\psi_1 = \tfrac{H_0\ I_0(x)\eta_z}{\Lambda}\Bigg(\ (\mu_1-\mu_2)\eta_z\left[\mu_2(K_0(b)+iK_1(b)\xi_z)\ (N_{ba}+iL_{ba}\eta_z+\ \xi_z\,(-iW_{ba}+N_{ba}\eta_z)\right]+ \\ \left[\mu_3(K_1(b)+iK_0(b)\eta_z)\,(W_{ba}+iN_{ab}\eta_z+\xi_z\,(-iN_{ba}+L_{ba}\eta_z)\right] - \tfrac{(\mu_2-\mu_3)\,\mu_2\xi_z(1+\eta_z^2)(K_0(b)+iK_1(b)\xi_z)}{a}\Bigg), \tag{2.23}$$

$$\psi_2 = \tfrac{H_0}{\Lambda}\,(K_0(x)(\mu_1-\mu_2)\,(I_0(a)-iI_1(a)\eta_z)\,[\mu_2\ (K_0(b)+iK_1(b)\xi_z)\ (I_1(a)\xi_z-(I_1(b)+i(I_0(a)-I_0(b))\xi_z)\eta_z)+ \\ \mu_3\,(-\ \xi_z(P_a^b+iV_a^b\xi_z)+i(P_a^b-G_b^b+iG_b^b\xi_z)\eta_z\xi_z-\ (E_b^b-iV_b^b\xi_z+E_a^b\xi_z^2)\eta_z] - \\ I_0(x)(\mu_2-\mu_3)\,(K_0(b)+iK_1(b)\xi_z)\times[\mu_2(iI_0(a)+I_1(a)\eta_z)\,(-iK_1(a)+(K_0(a)-K_0(b))\eta_z)\,\xi_z]+ \\ \mu_1\left(\eta_z(E_a^b-iG_a^b\eta_z)+\xi_z\left(P_a^a+i\left(P_a^b-P_a^a+V_a^a\right)\eta_z\ \ +N_{aa}\eta_z^2\right)\right)]) \tag{2.24}$$

and

$$\psi_3 = \tfrac{H_0\ K_0(x)\eta_z}{\Lambda}\,((\mu_3-\mu_2)\xi_z\left[\mu_2(I_0(a)-iI_1(a)\eta_z)\ (N_{ba}+iW_{ba}\eta_z+\ \xi_z\,(-iL_{ba}+N_{ba}\eta_z)\right]+ \\ \left[\mu_1(iI_1(a)+I_0(a)\eta_z)\,(-iW_{ba}+N_{ab}\eta_z-\xi_z\,(N_{ba}+iL_{ba}\eta_z)\right]+\tfrac{(\mu_1-\mu_2)\,\mu_2\eta_z(1+\xi_z^2)(I_0(a)-iI_1(a)\eta_z)}{b}\Big), \tag{2.25}$$

where $x = kr$, $a = kR_1$, $b = kR_2$ and N_{xb}, N_{ab}, W_{ax}, W_{bx}, W_{ba}, L_{ba}, E_a^b, G_a^b, P_a^b, V_a^b, E_b^a, G_b^a, P_b^a, V_b^a, E_a^a, G_a^a, P_a^a, V_a^a, E_b^b, G_b^b, P_b^b, V_b^b and Λ are given in the Appendix.

The distributions of the velocity and magnetic potentials contain nonlinear terms. As the nonlinear terms are ignored, the linear profile arises and equivalent to those obtained earlier by EL-Dabe et al. [11], and Rosensweig [28]. At this end, the boundary-value problem has been completed.

To analyze the stability of the system, the remaining boundary condition arises from the normal component of the stress tensor. In accordance with the presence of the amount of surface tensions, this normal component must be discontinuous. The total stress tensor can be formulated as follows:

$$\sigma_{ij} = -P\delta_{ij} + \mu H_i H_j - \frac{1}{2}\mu H^2 \delta_{ij} \tag{2.26}$$

where δ_{ij} is the Kronecker delta

$$\left\| \underline{n}_j . \underline{F}_j \right\| = T_i\, \nabla.\, \underline{n}_j, \qquad\qquad i, j = 1, 2 \tag{2.27}$$

where $\underline{F}_j$ is the total force acting on the interfaces, which is defined as

$$\underline{F} = \begin{pmatrix} \sigma_{rr} & \sigma_{rz} \\ \sigma_{zr} & \sigma_{zz} \end{pmatrix} \begin{pmatrix} n_r \\ n_z \end{pmatrix}, \tag{2.28}$$

here n_r, n_z are the components of the outward unit normal vector $\underline{n}$.

On substituting from the foregoing outcomes in Eq. (2.27), after lengthy but straightforward calculation, one gets the following nonlinear characteristic equations:

$$L_1\,\eta + L_2\,\xi = N_1(\eta, \xi), \tag{2.29a}$$

$$L_3\,\eta + L_4\,\xi = N_2(\eta, \xi), \tag{2.29b}$$

where the operator L_i is defined as $L_i = ia_i H_0^2 \frac{\partial}{\partial z} + b_i \frac{\partial^2}{\partial z^2} + c_i \frac{\partial^2}{\partial t^2}$. In addition, the nonlinear term $N_i(\eta, \xi)$ represents all the quadratic and cubic terms in the variables η, ξ and a_i, b_i and c_i are constants. They are all listed in the Appendix.

From the zero- order of the normal stress tensor, one gets

$$\lambda_2 - \lambda_1 = (\rho_2 - \rho_1)gz - \frac{T_1}{R_1} + \frac{1}{2}H_0^2(\mu_2 - \mu_1), \tag{2.30a}$$

$$\lambda_3 - \lambda_2 = (\rho_3 - \rho_2)gz - \frac{T_2}{R_2} + \frac{1}{2}H_0^2(\mu_3 - \mu_2)., \tag{2.30b}$$

It is worthwhile to conclude a special case from the previous coupled equations (2.29) as follows:

Returning to our previous work [29], on putting $V_1 = V_2 = 0$ and $\nu_1 = \nu_2 = 0$. This case can be obtained by setting, here, $\eta(z,t) = \xi(z,t)$, $R_1 = R_2$, $T_1 = T_2$ and then adding equations (2.29).

The stability analysis of the current work, throughout the linear as well as the nonlinear approach depends mainly on studying the nonlinear characteristic equations as given in equations (2.29). The following analysis will be based on our previous work [22].

3. The Linear Stability Approach

Before dealing with the general case, for more convenience, we will study the stability analysis throughout a linear point of view. In light of this approach, the linearized analysis of the nonlinear equations that are given by equations (2.29) arises when the nonlinear terms of the surface elevation are ignored.

Therefore, the linearized dispersion equations can be written as follows:

$$L_1\,\eta + L_2\,\xi = 0, \tag{3.1a}$$

$$L_3\,\eta + L_4\,\xi = 0. \tag{3.1b}$$

Suppose a uniform monochromatic wave train solution of equations (3.1) in the following form:

$$\eta(z,t) = \gamma_1\, e^{i(k\,z-\omega\,t)} + c.c., \tag{3.2a}$$

$$\xi(z,t) = \gamma_2\, e^{i(k\,z-\omega\,t)} + c.c.. \tag{3.2b}$$

where γ_1 and γ_2 are the amplitudes of the wave train solutions.

For the nontrivial solutions of γ_1 and γ_2 in equations (3.1), the determinant of the coefficient matrix must be cancelled. This concept gives the following dispersion relation:

$$\omega^4 + \alpha_1\omega^2 + \alpha_2 = 0, \tag{3.3}$$

where the coefficients α_1 and α_2 are listed in the Appendix.
Actually, the dispersion relation, which is a quadratic equation in ω^2. It is the same as that already had been achieved by Dumbleton, and Hermans [26] for the stability of a hollow perfect hollow cylinder. The former case may be obtained here by setting: $\rho_1 = \rho_3 = 0$, together with the absence of the magnetic field strength, i. e. $H_0 = 0$.

Eq. (3.3) represents a linear dispersion relation of the surface waves. The stability requires that all four roots of $\omega' s$ must be real, i. e. ω^2 should be of positive and real. On the basis of Eq. (3.3), it is easily verified that this implies the following criteria:

$$\alpha_1 < 0, \tag{3.4}$$

$$\alpha_2 > 0 \tag{3.5}$$

and

$$\alpha_1^2 - 4\alpha_2 > 0. \tag{3.6}$$

The attention is focused on the implication of the magnetic field strength on the stability configuration. Subsequently, the magnetic field intensity will be sketched versus the wave number k of the surface wave. Therefore, it is convenient to rewrite the stability criteria in term of the magnetic field strength H_0^2. Therefore, the inequalities (3.4)-(3.6) may be written as follows:

$$q_1 H_0^2 + q_0 < 0, \tag{3.7}$$

$$p_2 H_0^4 + p_1 H_0^2 + p_0 > 0 \tag{3.8}$$

and

$$w_2 H_0^4 + w_1 H_0^2 + w_0 > 0. \tag{3.9}$$

where the coefficients q_0, q_1, p_0, p_1, p_2, w_0, w_1, and w_2 are well-known from the context. They involved all the physical parameters of the problem.

The inspection of the conditions (3.7)-(3.9), reads that all of them depend on H_0^2. Before dealing with the numerical calculations, for more convenience, these stability conditions may be rewritten in an appropriate non-dimensional form. This can be done in a number of ways depending, basically, on the choice of characteristics of length, time and mass.

Consider that the parameters g/ω^2, $1/\omega$ and $\rho_2 g^3/\omega^6$ refer to the characteristics of length, time and mass, respectively. The other non-dimensional quantities may be given as
$\rho_j = \rho_j^* \rho_2$, $k = k^* \omega^2/g, H_0^2 = H_0^{*2} \rho_2 g^2/\omega^2 \mu_2$, $T_j = T_j^* \rho_2 g^3 \Big/ \omega^4$ and $R_j = R_j^* g/\omega^2$.

For simplicity, the " $*$ " mark may be cancelled in the following analysis.

The magnetic field intensity $Log\, H_0^2$ will be plotted versus the wave number of the surface waves$k$. Actually, the implication of the magnetic field strength depends mainly on the signs of the parameters of the leading coefficients of the previous criteria. Therefore, if p_2, and w_2 are positive, simultaneously, q_1 is negative, it follows that the magnetic field has a stabilizing influence. The numerical calculations ensure this significance. Therefore, the tangential magnetic field plays a stabilizing influence. Typically, this is an early result. It is first confirmed by many researchers; for instance, see [20, 29, 30].

In what follows, a numerical calculation is done to indicate the influence of various parameters on the stability configuration. Throughout the following figure, the transition curves that are appear in the inequalities (3.7) - (3.9), are plotted. In these figures, the stable region is referred by the letter S. Simultaneously, the letter U stands for the unstable one. The following calculations considered a sample chosen system, whose particulars are: $\rho_1 = 0.1$, $\rho_3 = 0.02, \mu_1 = 0.09, \mu_3 = 2, R_1 = 0.5$, $R_2 = 5$, $T_1 = 6$ and $T_2 = 10$. In accordance with these numerical values, it is found that the inequality (2.9) is automatically satisfied. Subsequently, it has no implication in the stability picture. Meanwhile, the first two inequalities (3.7) and (3.8) have three transition curves. Therefore, Fig. 2 is plotted to indicate these transition curves, as follows:

The equality of (3.7) is pictured in a dotted curve. Meanwhile, the equality of (3.8) is graphed to give two-solid curves. The calculations showed that q_1 is a negative. Therefore, the region above this curve is a stable region and is denoted by the letter S_1. In contrast, the region below this curve becomes an unstable region. It is referred by the letters U_1. On the other hand, the calculations showed that the leading coefficient p_2 has a positive sign. Consequently, the stable regions lie above the upper curve, together with the region below the lower curve. These regions are labeled by the letter S_2. Simultaneously, the region bounded between these two curves becomes an unstable region. It is referred by the letters U_2.

Mathematically, the equality of the relation (3.8) is a quadratic in H_0^2. Actually, it has two real and distinct roots, say H_1^* and H_2^*. Considering that $H_2^* > H_1^*$. In case of $p_2 > 0$, the stability occurs provided that $H_0^2 > H_2^*$ or $H_0^2 < H_1^*$. On the other hand, in case of $p_2 < 0$, the stability occurs provided that $H_1^* < H_0^2 < H_2^*$.

Consequently, Fig. 2 plots the three transition curves. As shown from the foregoing discussions, the stability of the system is judged by the upper solid curve. Therefore, the other two curves have no implication in the stability configuration. Subsequently, to indicate the influence of any parameter, it is enough to use only this judged curve.

Accordingly, Fig. 3 is plotted to show the influence of the sheet thickness on the stability configuration. For this purpose, the radius of the outer interface ($R_2 = 5.0$) is held fixed with a variation of the radius of the inner interface R_1 is done. The parameters of the chosen system here is the same as that is given in Fig. 2. As shown in this figure, the increase of sheet thickness leads to an increasing the stability region. Specially, at small values of the wave number. Actually, this shows a stabilizing influence of the sheet thickness in the stability configuration. This result is in agreement with the result that was already obtained by Moatimid [31]. Finally, Fig. 4 and 5 are depicted to indicate the influences of surface tensions T_1 and T_2. It was observed that T_1 and T_2 have destabilizing effects. These effects are enhanced, especially at large values of

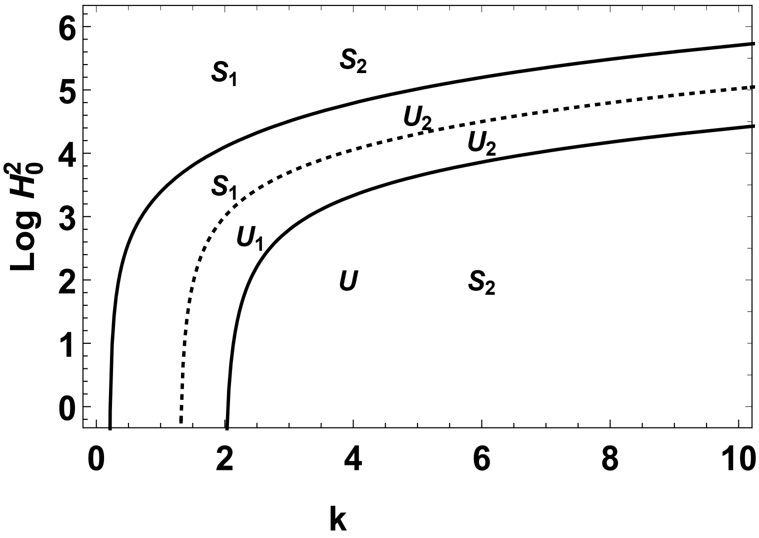

Figure 2: Plots the linear stability diagram as given in inequalities (3.7)-(3.9).

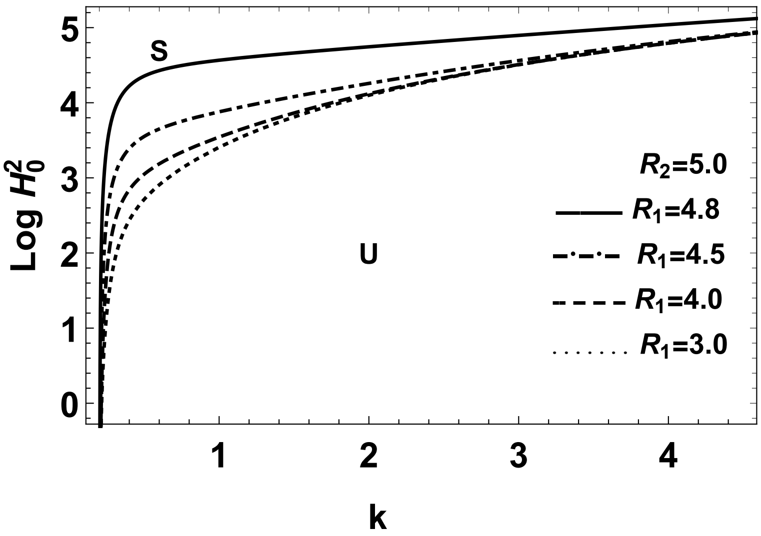

Figure 3: Plots the linear stability diagram as given in (3.7), for the variation of R_1

the wave number. These results are in correspondence of the previous results that were achieved by El-Sayed et al. [32], Li-Jun et al. [33] and Awasthi and Asthana [34].

To develop the nonlinear stability influence for the amplitude modulation of the progressive waves, we need to go to the full equations (2.29). The treatment of these equations may be achieved through the following perturbation technique.

4. The Nonlinear Stability Approach

The nonlinear stability procedure for equations (2.29) had been discussed in details throughout our previous work as given by El-Dib [22]. This work discussed the coupled nonlinear dispersion equations in a general form. Therefore, the current aim focuses on analyzing the nonlinear stability analysis of coupled cylindrical interfaces separating three different magnetic perfect fluids in the presence of an axial uniform

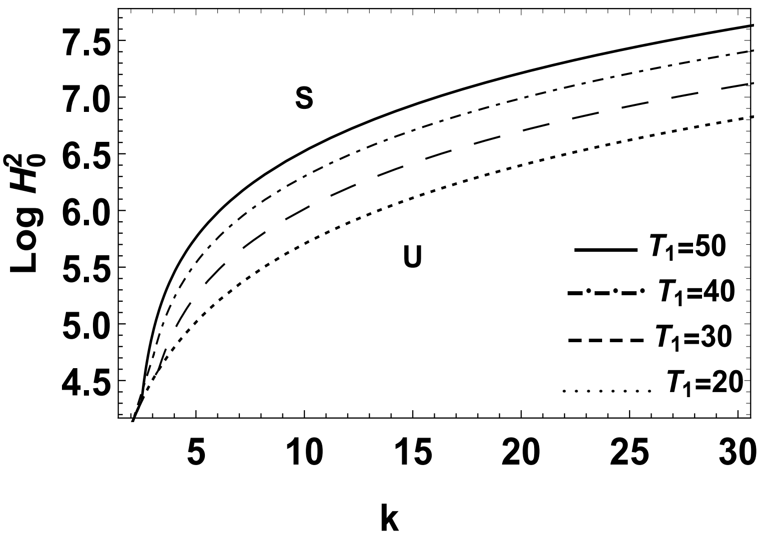

Figure 4: Plots the linear stability diagram as given in (3.7), for the variation of T_1

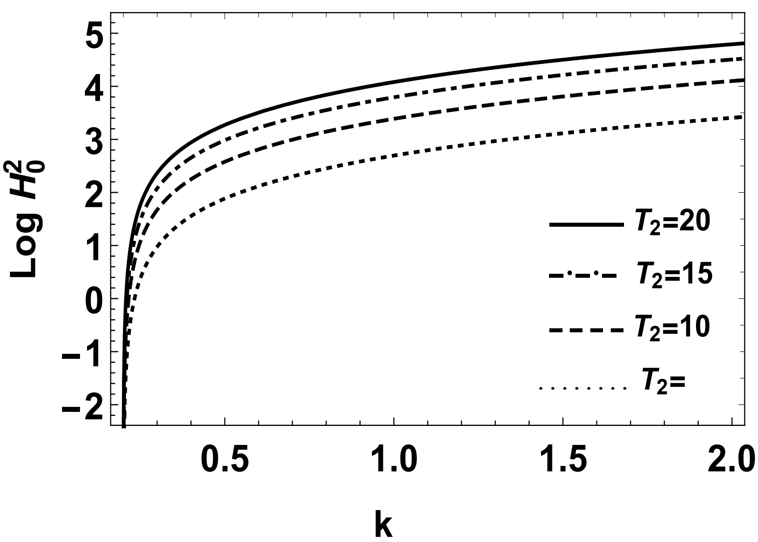

Figure 5: Plots the linear stability diagram as given in (3.7), for the variation of T_2

magnetic field. For this purpose, equations (2.29) may be rewritten in the following form:

$$\tilde{L}\,\eta = L_4N_1 - L_2N_2, \tag{4.1a}$$
$$\tilde{L}\,\xi = L_1N_2 - L_3N_1, \tag{4.1b}$$

where $\tilde{L} = L_1L_4 - L_2L_3$.

The following analysis will be based on the multiple time scale technique [18]. This technique depends mainly on a small parameter δ, say. It measures the ratio of a typical wave length, or periodic time, relative to a typical length, or the time scale of modulation. Therefore, one assume that δ be a small parameter that characterizes the slow modulation. In view of this approach, the independent variables z and t, which are measured on the scale of the typical wavelength and period time, can be extended to introduce alternative, independent variables,

$$Z_n = \delta^n z \qquad \text{and} \qquad T_n = \delta^n t, \qquad n = 0, 1, 2, ... \tag{4.2}$$

Considering $Z_0,\ T_0$ as the appropriate variables of fast variations and $Z_1,\ T_1,\ Z_2,\ T_2$ are the slow ones. The differential operators can now be expressed as the derivative expansions

$$\frac{\partial}{\partial z} = k\frac{\partial}{\partial \theta} + \delta\frac{\partial}{\partial Z_1} + \delta^2\frac{\partial}{\partial Z_2} + ...\text{and}\frac{\partial}{\partial t} = -\omega\frac{\partial}{\partial \theta} + \delta\frac{\partial}{\partial T_1} + \delta^2\frac{\partial}{\partial T_2} + ... \tag{4.3}$$

where $\theta = kZ_0 - \omega T_0$ refer to lowest order.

It is more convenient to expand the operator $\tilde{L}$ in the following form:

$$\tilde{L}\left(ik, -i\omega + i\delta\left(\frac{\partial}{\partial Z_1}, \frac{\partial}{\partial T_1}\right) + i\delta^2\left(\frac{\partial}{\partial Z_2}, \frac{\partial}{\partial T_2}\right) + ...\right). \tag{4.4}$$

The expression of the operator $\tilde{L}$ can be expanded in powers of δ. Using Taylor's theorem about $(k, -\omega)$, one retains only the terms up to $O(\delta^2)$. On that account,

$$\tilde{L} \to \tilde{L}_0 + \delta\,\tilde{L}_1 + \delta^2\tilde{L}_2 + ..., \tag{4.5}$$

where

$$\tilde{L}_0 \equiv (k, -\omega)\frac{\partial}{\partial \theta}, \tag{4.6a}$$
$$\tilde{L}_1 \equiv i\left(\frac{\partial \tilde{L}_0}{\partial \omega}\right)\frac{\partial}{\partial T_1} - i\left(\frac{\partial \tilde{L}_0}{\partial k}\right)\frac{\partial}{\partial Z_1}, \tag{4.6b}$$
$$\tilde{L}_2 \equiv i\left(\frac{\partial \tilde{L}_0}{\partial \omega}\right)\frac{\partial}{\partial T_2} - i\left(\frac{\partial \tilde{L}_0}{\partial k}\right)\frac{\partial}{\partial Z_2} - \frac{1}{2}\left(\frac{\partial^2 \tilde{L}_0}{\partial \omega^2}\right)\frac{\partial^2}{\partial T_1^2} - \frac{1}{2}\left(\frac{\partial^2 \tilde{L}_0}{\partial k^2}\right)\frac{\partial^2}{\partial Z_1^2} + \frac{1}{2}\left(\frac{\partial^2 \tilde{L}_0}{\partial k\,\partial \omega}\right)\frac{\partial^2}{\partial Z_1 \partial T_1}. \tag{4.6c}$$

Expressing the expansion of the operator (4.5) into Eq. (3.2), one gets

$$\left(\tilde{L}_0 + \delta\,\tilde{L}_1 + \delta^2\tilde{L}_2\right)(\eta, \xi) = 0, \tag{4.7}$$

The foregoing analysis follows a perturbation procedure to obtain a uniform valid solution. Actually, this treatment requires the cancellation of the secular terms. As stated before, this procedure was introduced in details by El-Dib [22]. On the other hand, it is well known that the coupled nonlinear Schrödinger equations are described in light of the unidirectional wave modulation. They have been used to describe the spatial and temporal evolution of the envelope of a sinusoidal wave with phase $(kz - \omega t)$. Therefore, following similar arguments as that was given by El-Dib [22], one finds the following coupled nonlinear Schrödinger equations:

$$i\frac{\partial \gamma_1}{\partial \tau} + P\frac{\partial^2 \gamma_1}{\partial \zeta^2} = \sum_{j=1}^{2} \left(Q_{1j}\gamma_j^2\overline{\gamma}_j + Q_{1j+1}\gamma_j^2\overline{\gamma}_{3-j} + Q_{1j+3}\gamma_1\gamma_2\overline{\gamma}_j \right), \tag{4.8a}$$

$$i\frac{\partial \gamma_2}{\partial \tau} + P\frac{\partial^2 \gamma_2}{\partial \zeta^2} = \sum_{j=1}^{2} \left(Q_{2j}\gamma_j^2\overline{\gamma}_j + Q_{2j+1}\gamma_j^2\overline{\gamma}_{3-j} + Q_{2j+3}\gamma_1\gamma_2\overline{\gamma}_j \right). \tag{4.8b}$$

where $\overline{\gamma}_j$ is the complex conjugate of γ_j,

$$P = \frac{1}{2}\frac{dV_g}{dk}, \qquad \zeta = \delta(z - V_g t), \qquad \tau = \delta^2 t,$$

the group velocity may be written as $V_g = -\frac{\partial D}{\partial k}\left(\frac{\partial D}{\partial \omega}\right)^{-1}$. and $Q_{i(j+n)}$ are constant coefficients. They will be known from the context. To avoid the lengthy of the paper, they will be omitted.

The stability criterion of the coupled nonlinear Schrödinger equations (4.8) has been derived from El-Dib [22]. He showed that the perturbation is stable in accordance with the following condition:

$$P\,S > 0, \tag{4.9}$$

where $S = L_2^2\left(Q_{11} + Q_{23} + Q_{25}\right) + L_1^2\left(Q_{14} + Q_{16} + Q_{22}\right).$

The condition (4.9) can be written as follows:

$$\frac{E_9(H_0^2)^9 + E_8(H_0^2)^8 + E_7(H_0^2)^7 + E_6(H_0^2)^6 + E_5(H_0^2)^5 + E_4(H_0^2)^4 + E_3(H_0^2)^3 + E_2(H_0^2)^2 + E_1 H_0^2 + E_0}{F_2 H_0^4 + F_1 H_0^2 + F_0} > 0, \tag{4.10}$$

where E_i and F_j are constant coefficients. They well-known from the context. To avoid the lengthy of the paper, they will be omitted.

The stability criterion requires that the quotient in the L. H. S. in the inequality (4.10) must be positive. This may be occurring if the product of the numerator and denominator becomes a positive. Subsequently, in light of the nonlinear theory approach, the system is stable provided that the following condition holds:

$$(E_9(H_0^2)^9 + E_8(H_0^2)^8 + E_7(H_0^2)^7 + E_6(H_0^2)^6 + E_5(H_0^2)^5 + E_4(H_0^2)^4 + E_3(H_0^2)^3 + E_2(H_0^2)^2 + E_1 H_0^2 + E_0 > 0, \tag{4.11a}$$

which is a polynomial of the eleventh degree in H_0^2.

In addition, one finds the following criterion:

$$F_2 H_0^4 + F_1 H_0^2 + F_0 = 0. \tag{4.11b}$$

The condition (4.11b) is sometimes called the resonance curves.

Otherwise, the system becomes unstable.

Now, for more convenience, a numerical calculation of the stability criteria as is given by the relations (4.11) will be made. For this purpose, consider a similar treatment as presented in Section 3 to evaluate the above stability criteria in a non-dimensional form. Therefore, one may assume the previous characteristics that were given in Section 3.

In order to illustrate the stability criteria throughout the nonlinear stability approach. Typically, it is convenient to graph $LogH_0^2$ versus the wave number of the surface waves (k). As previously shown, the stable region is referred by the letter S. Simultaneously, the letter U stands for the unstable one.

Fig. 6 plots the transition curves (4.11). The following calculations considered a chosen sample system, whose particulars are:

$\rho_1 = 2$, $\rho_3 = 5$, $\mu_1 = 3$, $\mu_3 = 5, R_1 = 0.01$, $R_2 = 0.1$, $T_1 = 5$ and $T_2 = 50$. In accordance with this numerical choice, the polynomial of the eleventh degree in H_0^2, as given in (49I), resulted in only three real positive roots of H_0^2. Simultaneously, the resonance curves, as showed in (4.11b), yielded two real positive roots for H_0^2. Fortunately, the other two roots are coincident with two of three of the previous cases. As seen, the stability diagram is portioned into four alternate regions of stability/instability. This is in contrast with the

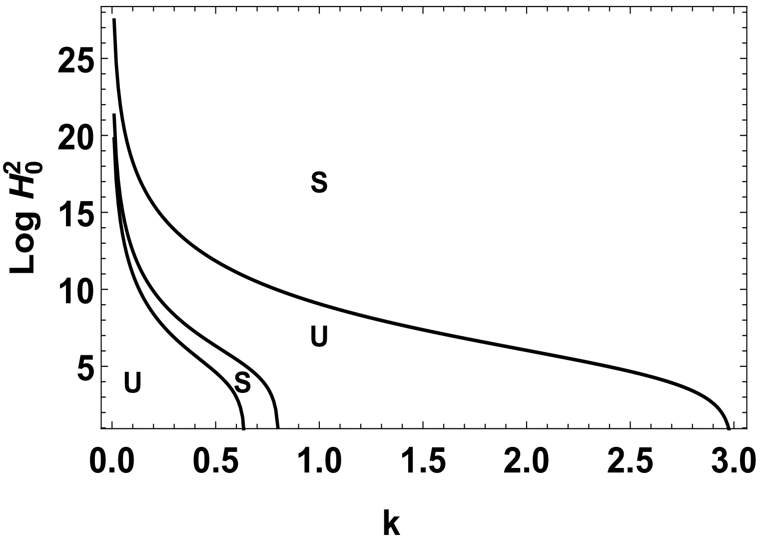

Figure 6: Plots the nonlinear stability diagram as given in (4.11a).

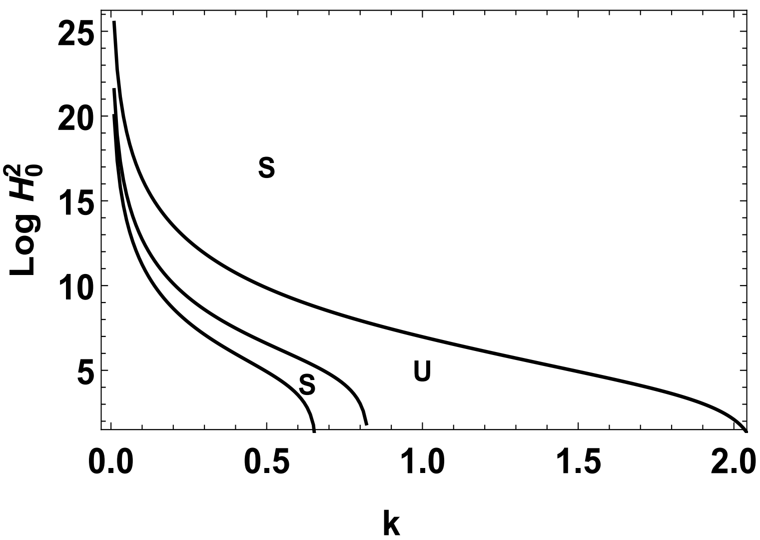

Figure 7: Plots the nonlinear stability diagram as given in (4.11a).

linear approach. Therefore, the nonlinear stability analysis gives more accuracy. To confirm the previous conclusion, finally, Fig. 7 is plotted for the transition curves (4.10) to show what is happening when R_1 changed. The chosen system here is the same as that is given in Fig. 6 but with a difference $R_1 = 0.05$. A comparison between the two curves shows that the increasing of the radius of the inner radius plays a stabilizing role in the stability picture. Therefore,the nonlinear stability shows an in contrast mechanism of the role of the sheet thickness.

5. Concluding Remarks

The current paper investigates the linear, as well as nonlinear stability analysis of two cylindrical interfaces, separated three perfect, homogeneous, and incompressible magnetic fluids. The system is influenced by a uniform axial magnetic field. As given by our foregoing papers; see, for instance, Refs. [23, 29], the nonlinear approach is derived from the linear solutions of the governing equations of motion together with the appropriate nonlinear boundary conditions. To relax the mathematical manipulation, a simplified formulation is considered to yield coupled characteristic nonlinear partial differential equations of the deflections of the surface waves without any complex coefficients. The case of the nonlinear stability of a single interface as was given by Moatimid [29] is recovered. As a special case, when ignoring the nonlinear terms, the linear stability criteria have been obtained. The limiting case of the linear stability analysis of the coupled interfaces as was given by Dumbleton and Hermans [26] is, also, recovered. In addition, the special case of the linear coupled interfaces that was given by El-Dabe et al. [11] is furthermore obtained. The numerical calculations, throughout the linear approach, confirmed similar results as that were given by many researchers. Following similar arguments that were given by El-Dib [22], it follows that the stability criteria are judged. Consequently, the nonlinear characteristic equations are analyzed along the utilizing nonlinear Schrödinger equation. These equations are controlled by the nonlinear stability criterion of the system. These conditions are illustrated graphically throughout a set of figures. The influences of some physical parameters had been shown. The concluding remarks may be drawn along the following points:

* The investigation of the linear stability analysis yields the following:

* Away from the interface of a single interface, the current case resulted in a quadratic equation of the square of the growth rate of the surface waves.

* The linear dispersion relation is given by Eq. (3.3). This equation resulted in several transition cures.

* As given by Moatimid [31], it is found that the increase in the sheet thickness plays a stabilizing influence on the stability configuration.

* The influence of the amounts of the surface tensions T_1 and T_2 play a destabilizing effect. This result is in correspondence with the previous results that were achieved by El-Sayed et al. [32], Li-Jun et al. [33] and Awasthi and Asthana [34].

* The analysis of the nonlinear stability analysis results in the following:

* The analysis yields coupled nonlinear characteristic equations as appearing in equations (2.29).

* Following our previous work as given by El-Dib [22], one finds the coupled nonlinear Schrödinger equation as given in equations (4.8).

* The transition curves yields a polynomial of the eleventh degree in H_0^2. Together with resonance quadratic polynomial in H_0^2.

* The numerical calculations in light of a chosen sample system, divides the stability picture into several parts of stability/instability.

* The nonlinear stability shows an in contrast mechanism of the role of the sheet thickness.

References

[1] B. Berkovski and V. Bashtovoy, *Magnetic Fluids and Applications Hndbook*, Begel House, New York, 1996.

[2] T. Rheinländer, R. Kötitz, W. Weitschies and W. Semmler, *Magnetic fluids: biomedical applications and magnetic fractionation*, Magnetic and Electrical Separation, 10(2000) 179-199.

[3] R.N. Chaniyilparampu, P. Kopčanský and R.V. Mehta, *Applications of magnetic fluids in medicine and biotechnology*, Indian J. Pure Ap. Phy., 39 (2001) 683-686.

[4] S. Mornet, S. Vasseur, F. Grasset and E. Duguet, *Magnetic nanoparticle design for medical diagnosis and therapy*, J. Mater. Chemistry, 14 (2004) 2161-2175.

[5] R. Ganguly, A.P. Gaind, S. Sen and I.K. Puri, *Analyzing ferrofluid transport for magnetic drug targeting*, J. Magn. Magn. Mater., 289 (2005) 331-334.

[6] C. Scherer and A.M.F. Neto, *Ferrofluids: Properties and Applications*, Braz. J. Phys., 35 (2005) 718-727.

[7] S. Chandrasekhar, *Hydrodynamic and Hydromagnetic Stability*, Clarendon Press, Oxford, 1961.

[8] S.F. El Shehawey, Y.O. El-Dib and A.A. Mohamed, *Electrohydrodynamic stability of a fluid layer: Effect of a tangential field*, IL Nuovo Cimento D, 6 (1985) 291-308.

[9] A.A. Mohamed, E.F. El Shehawey and Y.O. El Dib, *Electrohydrodynamic stability of a fluid layer: Effect of a tangential periodic field*, IL Nuovo Cimento, 8 (1986) 177-192.

[10] A.A. Mohamed, E.F. El Shehawey and Y.O. El Dib, *Electrohydrodynamic stability of a fluid layer:II. Effect of a normal field*, J. Chem. Phys., 85 (1986) 445-455.

[11] N.T. El-Dabe, E.F. El Shehawey, G.M. Moatimid and A.A. Mohamed, *Electrohydrodynamic stability of two cylindrical interfaces under influence of a tangential periodic field*, J. Math. Phys., 26 (1985) 2072-2081.

[12] Y.O. El-Dib and R.T. Matoog, *Stability of streaming in an electrified Maxwell fluid sheet influenced by a vertical periodic field in the absence of surface charges*, J. Colloid Interface Sci., 229 (2000) 29-52.

[13] G.M. Moatimid, Y.O. El-Dib and M.H. Zekry, *Stability analysis using multiple scales homotopy approach of coupled cylindrical interfaces under the influence of periodic electrostatic fields*, Chinese J. Phys., 56 (2018) 2507-2522.

[14] G.M. Moatimid, Y.O. El-Dib and M.H. Zekry, *Instability analysis of a streaming electrified cylindrical sheet through porous media*, Pramana J. Phys., 92:22 (2019).

[15] A. Arnold, *Numerically absorbing boundary conditions for quantum evolution equations*, VLSI Design, 6 (1998) 313-319.

[16] M. Levy, *Parabolic Equation Methods for Electromagnetic Wave Propagations*, IEEE, (2000).

[17] G. Arora, V. Joshi, and R.C. Mittal, *Numerical simulation of nonlinear Schrödinger equation in one and two dimensions*, Math. Models Comp. Simulations, 11 (2019) 634-648.

[18] A.H. Nayfeh, *Nonlinear propagation of wave packets on fluid interfaces*, J. Appl. Math., ASME 98E (1976) 584-588.

[19] A.F. Elhefnawy, *The nonlinear stability of mass and heat transfer in magnetic fields*, ZAMM, 77 (1997) 19-31.

[20] D.S. Lee, *Nonlinear stability in magnetic fluids of cylindrical interface with mass and heat transfer*, Eur. Phys. J. B, 28 (2002) 495-503.

[21] K. Zakaria, *Nonlinear dynamics of magnetic fuids with a relative motion in the presence of an oblique magnetic field*, Physica A, 327 (2003) 221-248.

[22] Y.O. El-Dib, *Nonlinear wave-wave interaction and stability criterion for parametrically coupled nonlinear schrödinger equations*, Nonlinear Dynam., 24 (2001) 399-418.

[23] G.M. Moatimid, *Non-linear electrorheological instability of two streaming cylindrical fluids*, J. phys. A Math. Gen., 36 (2003) 11343-11365.

[24] A.F. Elhefnawy, G.M. Moatimid and A.K. Elcoot, *Nonlinear electrohydrodynamic instability of a finitely conducting cylinder: Effect of interfacial surface charges*, ZAMP, 55 (2004) 63-91.

[25] G.M. Moatimid, Y.O. El-Dib and M.H. Zekry, *The nonlinear instability of a cylindrical interface between two hydromagnetic Darcian flow*, Arab J. Sci. Eng., 45 (2020) 391–409.

[26] J.H. Dumbleton and J.J. Hermans, *Capillary stability of a hollow inviscid cylinder*, Phys. Fluids, 13 (1970) 12-17.

[27] J.R. Melcher, *Field Coupled Surface Waves*, MIT Press, Cambridge 1963.

[28] R.E. Rosensweig, *Ferrohydrodynamic*, Cambridge University Press, Cambridge, 1985.

[29] G.M. Moatimid, *Nonlinear waves on the surface of a magnetic fluid jet in porous media*, Physica A, 328 (2003) 525-544.

[30] M. D. Cowley and R. E. Rosensweig, *The interfacial stability of a ferromagnetic fluid*, J. Fluid Mech., 30 (1968) 671-688.

[31] G.M. Moatimid, *Stability conditions of an electrified miscible viscous fluid sheet*, J. Colloid Interface Sci., 259 (2003) 186-199.

[32] M.F. El-Sayed, G.M. Moatimid and T.M.N. Metwaly, *Nonlinear electrohydrodynamic stability of two superposed streaming finite dielectric fluids in porous medium with interfacial surface charges*, Transport in Porous Med., 86 (2011) 559-578.

[33] Y. Li-Jun Y., D. Ming-Long, F. Qing-Fei and Z. Wei, *Linear stability analysis of a power-law liquid jet*, Atomization Sprays, 22 (2012) 123-141.

[34] M.K. Awasthi and R. Asthana, *Viscous potential flow analysis of capillary instability with heat and mass transfer through porous media*, Int. Commun. Heat Mass Tran., 40 (2013) 7-11.

Appendix

The coefficients that appear in Eqs. (2.20)-(2.25) may be listed as follows:

$$N_{ab} = I_0(a)K_1(b) + I_1(b)K_0(a), N_{ax} = I_0(a)K_1(x) + I_1(x)K_0(a), N_{bx} = I_0(b)K_1(x) + I_1(x)K_0(b),$$

$$N_{ba} = I_0(b)K_1(a) + I_1(a)K_0(b),\ L_{ab} = I_1(a)K_1(b) - I_1(b)K_1(a),\ L_{ba} = I_1(b)K_1(a) - I_1(a)K_1(b),$$

$$W_{ab} = I_0(a)K_0(b) - I_0(b)K_0(a),\ W_{ax} = I_0(a)K_0(x) - I_0(b)K_0(x),\ W_{bx} = I_0(b)K_0(x) - I_0(x)K_0(b),$$

$$P_a^b = I_0(a)K_0(b),\ P_a^a = I_0(a)K_0(a),\ P_b^b = I_0(b)K_0(b),\ P_b^a = I_0(b)K_0(a),$$

$$V_a^b = I_1(a)K_1(b),\ V_a^a = I_1(a)K_1(a), V_b^b = I_1(b)K_1(b), V_b^a = I_1(a)K_1(b),$$

$$E_a^b = I_0(a)K_1(b),\ \ E_a^a = I_0(a)K_1(a),\ \ E_b^b = I_0(b)K_1(b),\ \ E_b^a = I_0(b)K_1(a),$$

and

$$G_a^b = I_1(a)K_0(b),\ G_a^a = I_1(a)K_0(a),\ G_b^b = I_1(b)K_0(b),\ G_b^a = I_1(b)K_0(a).$$

The coefficients that appear in Eqs. (29I, and 29II) may be listed as follows:

$$L_1 = ia_1 H_0^2 \frac{\partial}{\partial z} + b_1 \frac{\partial^2}{\partial z^2} + c_1 \frac{\partial^2}{\partial t^2},$$

$$a_1 = -2a(\mu_1-\mu_2)^2 k^3 I_0(a) L_{ba} \left[\mu_2^2 P_a^b V_b^a + \mu_2\mu_3\, U_{ab}^{ab} + \mu_1\mu_2\, D_{ab}^{ab} + (\mu_1-\mu_2)(\mu_2-\mu_3) P_a^b V_b^b + \mu_1\mu_3 P_b^a V_a^b\right] \left[\mu_2 G_b^a G_a^b + (\mu_2-\mu_3) G_a^b V_a^b + \mu_3 P_b^a V_a^b\right],$$

$$b_1 = -2aT_1 k^3 I_1(a) L_{ba} \left(\mu_2^2 P_a^b V_b^a + \mu_2\mu_3\, E_a^a E_b^b + \mu_1\mu_2 G_a^a G_b^b + (\mu_1-\mu_2)(\mu_2-\mu_3) P_a^b V_a^b + \mu_1\mu_3 P_b^a V_a^b\right)^2,$$

$$c_1 = -2ak^2 \left[\mu_1 \left(\mu_2 G_a^b N_{ab} + \mu_3 V_a^b W_{ba}\right) + \mu_2 \left(\mu_2 P_a^b L_{ba} + \mu_3 E_a^b N_{ba}\right)\right]^2 \left[\rho_1 I_0(a) L_{ab} - \rho_2 I_1(a) L_{ba}\right],$$

$$L_2 = ia_2 H_0^2 \frac{\partial}{\partial z} + b_2 \frac{\partial^2}{\partial z^2} + c_2 \frac{\partial^2}{\partial t^2},$$

$$a_2 = -2a(\mu_1-\mu_2)(\mu_2-\mu_3)\mu_2 k^3 I_0(a) I_1(a) L_{ba} \left[\mu_2^2 P_a^b V_b^a + \mu_2\mu_3 E_a^a E_b^b + \mu_1\mu_2\, G_a^a G_b^b + \mu_1\mu_3 P_b^a V_a^b + (\mu_1-\mu_2)(\mu_2-\mu_3) P_a^b V_b^b\right], \qquad b_2 = 0,$$

$$c_2 = -2\rho_1 k^2 I_1(a) \left[\mu_2^2 P_a^b V_b^a + \mu_2\mu_3\, E_a^a E_b^b + \mu_1\mu_2\, G_a^a G_b^b + (\mu_1-\mu_2)(\mu_2-\mu_3) P_a^b V_a^b + \mu_1\mu_3 P_b^a V_a^b\right]^2,$$

$$L_3 = ia_3 H_0^2 \frac{\partial}{\partial z} + b_3 \frac{\partial^2}{\partial z^2} + c_3 \frac{\partial^2}{\partial t^2},$$

$$a_3 = -2a(\mu_1-\mu_2)(\mu_2-\mu_3)\mu_2 k^3 K_1(b) P_a^b L_{ba} \left[\mu_2^2 P_a^b V_b^a + \mu_2\mu_3\, E_a^a E_b^b + \mu_1\mu_2\, G_a^a G_b^b + \mu_1\mu_3 P_b^a V_a^b + (\mu_1-\mu_2)(\mu_2-\mu_3) P_a^b V_b^b\right], \qquad b_3 = 0,$$

$$c_3 = -2\rho_2 k^2 K_1(b) \left[\mu_2^2 P_a^b V_b^a + \mu_2\mu_3\, E_a^a E_b^b + \mu_1\mu_2 G_a^a G_b^b + (\mu_1-\mu_2)(\mu_2-\mu_3) P_a^b V_a^b + \mu_1\mu_3 P_b^a V_a^b\right]^2,$$

$$L_4 = ia_4 H_0^2 \frac{\partial}{\partial z} + b_4 \frac{\partial^2}{\partial z^2} + c_4 \frac{\partial^2}{\partial t^2},$$

$$a_4 = 2b(\mu_2-\mu_3)^2 k^3 K_0(a) L_{ab} \left[\mu_2^2 P_a^b V_b^a + \mu_2\mu_3\, E_a^a E_b^b + \mu_1\mu_2\, G_a^a G_b^b + (\mu_1-\mu_2)(\mu_2-\mu_3) P_a^b V_b^b + \mu_1\mu_3 P_b^a V_a^b\right] \left[\mu_1 P_b^a V_a^b + (\mu_2-\mu_1) G_a^b V_a^a + \mu_2 E_a^a E_b^a\right],$$

$$b_4 = 2bT_2 k^3 K_1(b) L_{ab} \left(\mu_2^2 P_a^b V_b^a + \mu_2\mu_3\, E_a^a E_b^b + \mu_1\mu_2\, G_a^a G_b^b + (\mu_1-\mu_2)(\mu_2-\mu_3) P_a^b V_b^b + \mu_1\mu_3 P_b^a V_a^b\right)^2,$$

$$c_4 = 2bk^2 \left[\mu_2^2 P_a^b V_b^a + \mu_2\mu_3\, E_a^a E_b^b + \mu_1\mu_2\, G_a^a G_b^b + (\mu_1-\mu_2)(\mu_2-\mu_3) P_a^b V_b^b + \mu_1\mu_3 P_b^a V_a^b\right]^2 \left[\rho_2 K_1(b) N_{ba} + \rho_3 K_0(b) L_{ab}\right],$$

$$N_1(\eta,\xi) = N_{11m}\eta_{tt}\xi_z + N_{12m}\eta_z\xi_{tt} + N_{13m}\xi_z^2 + N_{14m}\eta_z\eta_{tt} + N_{15m}\xi_z\eta_{zz} + N_{16m}\xi_z\xi_{tt} + N_{17m}\eta_z\eta_{zz} + N_{18m}\eta_z\xi_z + N_{19m}\,\eta_z^2 + N_{11n}\xi_{tt}\xi_z^2 + N_{12n}\eta_{tt}\xi_z^2 + N_{13n}\xi_z^3 + N_{14n}\xi_{tt}\xi_z\eta_z + N_{15n}\eta_{tt}\xi_z\eta_z + N_{16n}\eta_z\xi_z^2 + N_{17n}\xi_{tt}\eta_z^2 + N_{18n}\eta_{tt}\eta_z^2 + N_{19n}\,\xi_z\eta_z^2 + N_{110n}\,\eta_z^3 + N_{111n}\,\eta_{zz}\xi_z^2 + N_{112n}\,\eta_z\eta_{zz}\xi_z + N_{113n}\,\eta_{zz}\eta_z^2$$

and

$$N_2(\eta,\xi) = N_{21m}\xi_{tt}\eta_z + N_{22m}\eta_z\xi_{tt} + N_{23m}\eta_z^2 + N_{14m}\eta_z\eta_{tt} + N_{15m}\xi_z\eta_{zz} + N_{16m}\xi_z\xi_{tt} + N_{17m}\eta_z\eta_{zz} + N_{18m}\eta_z\xi_z + N_{19m}\xi_z^2 + N_{21n}\eta_{tt}\eta_z^2 + N_{22n}\xi_{tt}\eta_z^2 + N_{23n}\eta_z^3 + N_{24n}\eta_{tt}\eta_z\xi_z + N_{25n}\xi_{tt}\eta_z\xi_z + N_{26n}\xi_z\eta_z^2 + N_{27n}\eta_{tt}\xi_z^2 + N_{28n}\xi_{tt}\xi_z^2 + N_{29n}\,\eta_z\xi_z^2 + N_{210n}\,\xi_z^3 + N_{211n}\,\xi_{zz}\eta_z^2 + N_{212n}\,\xi_z\xi_{zz}\eta_z + N_{213n}\,\xi_{zz}\xi_z^2,$$

where N_{ijn} and N_{ijm} $(i = 1,2)$, $(\,j = 1,2,.....13)$ are constant coefficients well-known from the context. To avoid the lengthy of the paper, they will be omitted.

The coefficients that appear in Eq. (3.3) may be listed as follows:

$$\alpha_1 = \frac{kH_0^2\left(a_2c_3 + a_3c_2 - a_1c_4 - a_4c_1\right) + b_1c_4 - b_4c_1}{c_1c_4 - c_2c_3},$$

and

$$\alpha_2 = \frac{\left(ka_1H_0^2 - b_1k^2\right)\left(ka_4H_0^2 - b_4k^2\right) + a_2a_3k^2H_0^2}{c_1c_4 - c_2c_3}.$$